Molecular Dynamics Simulation of a Double-Helical β-Carrageenan Hexamer Fragment in Water

K. Ueda*

Department of Physical Chemistry, Faculty of Engineering, Yokohama National University, 79-5 Tokiwadai, Hodogaya-ku, Yokohama 240-8501, Japan

A. Imamura

Department of Chemistry, Faculty of Science, Hiroshima University, Kagamiyama, Higashi-Hiroshima 739, Japan

J. W. Brady*

Department of Food Science, Stocking Hall, Cornell University, Ithaca, New York 14853

Received: July 16, 1997; In Final Form: February 18, 1998

Molecular dynamics simulations were conducted of two hexasaccharide strands of β-carrageenan in aqueous (TIP3P) solution in the double-helical conformation proposed for ι-carrageenan from fiber diffraction experiments. A similar simulation was performed for the complex in vacuum as a theoretical control. In the vacuum simulation the individual chains made conformational transitions, but the complex remained a double helix overall, apparently owing to the persistence of the stabilizing interchain hydrogen bonds. In the solution simulations, however, these interchain hydrogen bonds did not persist, but rather exchanged for hydrogen bonds to solvent, and possibly as a result, the double helix was observed to begin to unravel. However, the individual glycosidic linkages in the separate strands appear to be more stable in the fiber diffraction conformation in solution than in the vacuum simulation, suggesting that the polysaccharide exists in solution as a single helix with approximately the same conformation as previously proposed for these chains in the double helix.

Introduction

The carrageenans are a family of commercially important polysaccharides extracted from marine red algae.[1] The basic structure of these polymers consists of repeating units of β-D-galactose and 3,6-anhydro-α-D-galactose. These chains are generally sulfated, with the various members of the carrageenan family differing in the details of this sulfation. Because carrageenans can form useful thermoreversible gels, much work has been directed toward investigating their properties, including their hydration behavior, solution conformations, and gelation mechanisms. In spite of these efforts, the conformations of the carrageenans in solution are still a matter of debate. X-ray fiber diffraction experiments have been interpreted to imply that in gels κ- and ι-carrageenan have double-helical conformations,[2−4] and a number of studies have been published which suggest that the conformation in solution is double-helical as well.[5−9] In contrast to these models, Smidsrod and co-workers have proposed a single helix structure for the ordered portions of carrageenan gels,[10−12] and Vanneste et al. have reported that ι-carrageenan in NaI and NaCl solutions exists in a single helical conformation by using low-angle laser light scattering experiments.[13] Hjerde et al. have recently described acid hydrolysis experiments consistent with the possibility of a double-helical solution state, in contrast to their previous reports of the existence of a single-helical state.[14]

Theoretical molecular mechanics (MM) simulations have also been used to study the conformations of carrageenans. There have been several conformational energy studies of the disaccharide repeat units,[15−18] and in two previous papers we have reported molecular dynamics (MD) simulations of the unsulfated β-carrageenan disaccharides in aqueous solution.[19,20] These various MM studies have involved several different computational approaches and empirical energy functions but have nonetheless produced results in relatively good agreement with one another and with experiment. Unfortunately, these previous MM studies have also not been able to resolve the question of whether the carrageenans are single or double helices in solution. The helix−coil transition for carrageenan depends on various conditions, such as the sulfate content, degree of polymerization, polymer concentration, temperature, and added salt ion concentration, which greatly complicate theoretical modeling calculations. It is also true that double-helical polymers may experience a number of long-range interactions along the chains and specific stabilizing forces between the chains, such as interchain hydrogen bonds, which would not be present in disaccharide calculations. It might thus be useful to directly simulate the solution behavior of a larger oligomeric fragment of the polymer.

In an attempt to explore the short-term dynamics of carrageenan helices, we report here MD simulations of a hexamer fragment of the double-helical β-carrageenan in vacuum and in aqueous solution. This unsulfated polysaccharide is not found in nature but serves as a useful model for many of the conformational features of this general class of polymers. The hexamer fragments simulated here correspond to the two-residue fragments of the double-helical structure obtained from the fiber

S1089-5639(97)02317-7 CCC: $15.00 © 1998 American Chemical Society
Published on Web 03/31/1998

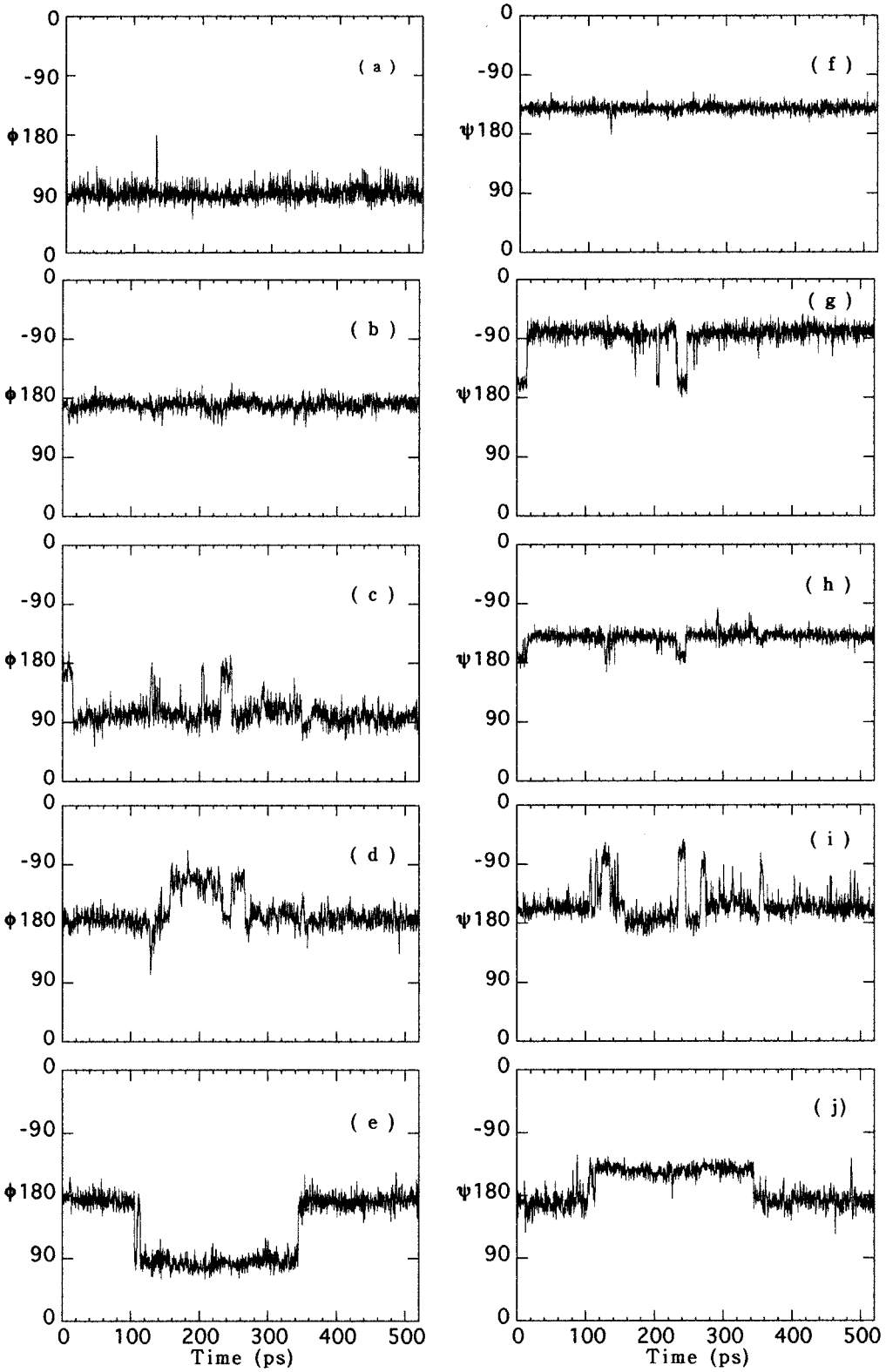

Figure 1. History of the glycosidic dihedral angles ϕ (a−e) and ψ (f−j) of strand 1 in the vacuum simulation: (a) and (f) A1(1→3)B2, (b) and (g) B2(1→4)A3, (c) and (h) A3(1→3)B4, (d) and (i) B4(1→4)A5, (e) and (j) A5(1→3)B6.

X-ray diffraction experiments of Arnott et al.[3] The helix−coil transition is a cooperative process that depends on the length (DP) of the polymer. Although the hexamer fragment considered here is probably too short to obtain a clear resolution of the problem of the helical structure of carrageenan, it can provide useful molecular-level information about the interaction between the strands of carrageenan molecules and between the carrageenan molecule and solvent water.

Procedures

In the present modeling calculations the starting structure of the β-carrageenan hexamer dimer was taken from the conformation of double-helical ι-carrageenan proposed from fiber X-ray diffraction by Arnott et al.[3] This structure was slightly modified in the same manner as in previous studies[19] by removing the sulfate residues from the O2 position of the 3,6-anhydro-α-D-

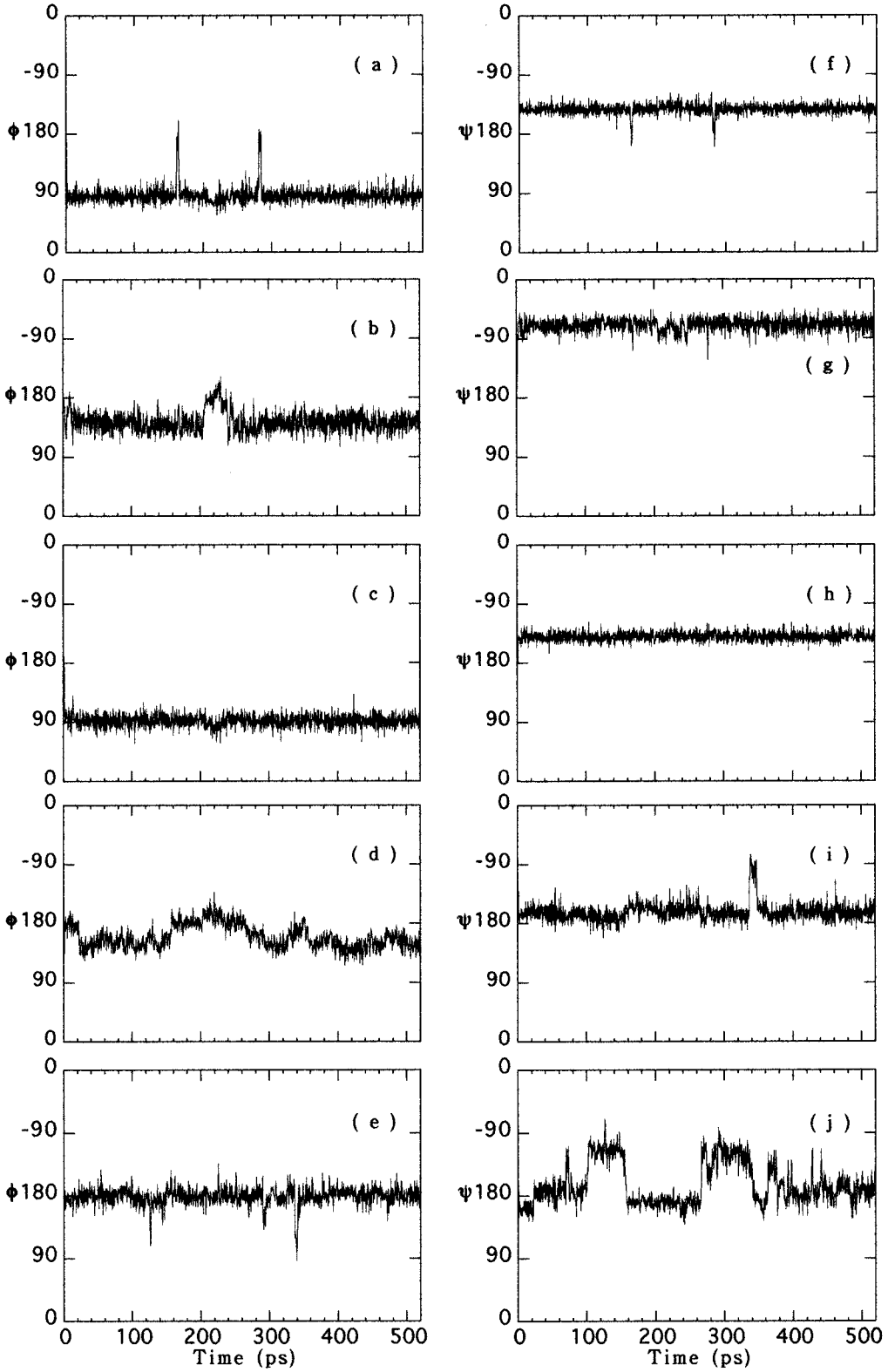

Figure 2. History of the dihedral angles ϕ and ψ of strand 2 in the vacuum simulation, as in Figure 1: (a) and (f) A′1(1→3)B′2, (b) and (g) B′2(1→4)A′3, (c) and (h) A′3(1→3)B′4, (d) and (i) B′4(1→4)A′5, (e) and (j) A′5(1→3)B′6.

galactose residues and the O4 position of the β-D-galactose residues in ι-carrageenan and replacing them with hydroxyl groups. For simplicity, in what follows the 3,6-anhydro-α-D-galactopyranose rings will be designated by the letter A, and the β-D-galactopyranose rings will be designated by the letter B. Using the above nomenclature, one of the hexamer strands of β-carrageenan can be written, starting from the nonreducing end, as A1(1→3)B2(1→4)A3(1→3)B4(1→4)A5(1→3)B6. The residues for the second strand will be indicated with primes as A′1(1→3)B′2(1→4)A′3(1→3)B′4(1→4)A′5(1→3)B′6. The designations "first" and "second" are of course arbitrary since the chains are identical. The glycosidic torsion angles ϕ and ψ for (1→3) linkages in strand 1 will be defined here in terms of the carbon and oxygen atoms of the linked monomers as AnC2−AnC1−B(n + 1)O1−B(n + 1)C3 and AnC1−B(n + 1)O1−B(n + 1)C3−B(n + 1)C2, respectively, where the letter n can

take the values 1, 3, and 5. Here the letter and number preceding each atom designation (C or O) indicate the sugar residue number, and the number following the atom designation indicates the atom position in each residue. For (1→4) linkages, the angles ϕ and ψ are defined as B*m*C2−B*m*C1−B*m*O1−A(*m* + 1)C4 and B*m*C1−B*m*O1−A(*m* + 1)C4−A(*m* + 1)C3, respectively, where the letter *m* takes the values 2 and 4. For strand 2 a prime will be placed on the above residue names. In the proposed fiber diffraction structure of ι-carrageenan, these glycosidic angles are (−163°, −159°) and (155°, −159°) for the (1→3) and (1→4) linkages, respectively.

Two separate MD simulations were carried out; one of a double-helical hexamer fragment in aqueous solution and one of this same oligosaccharide dimer in vacuum as a control. All calculations were performed using the general molecular mechanics program CHARMM[21] and potential parameters developed for carbohydrate molecules.[22] Trajectories were integrated using a Verlet algorithm,[23] and the SHAKE procedure[24] was used to keep bond lengths involving hydrogen atoms fixed and to maintain the rigidity of the water molecules. In the vacuum simulation the double helix was randomly assigned initial atomic velocities from a Boltzmann distribution at a temperature of 60 K and heated to 300 K by periodic reassignments over a period of 10 ps, after which it was equilibrated at 300 K for an additional 10 ps, during which time the atomic velocities were scaled if the temperature deviated by more than ±3 K from 300 K. Following this heating and equilibration, the trajectory was integrated for an additional 500 ps for the purpose of data collection. In the solution simulation, periodic boundary conditions were used with a primary box size of 30.7 Å × 30.7 Å × 46.2 Å containing 1384 TIP3P water molecules,[25,26] which gives a density of 1.026 g/cm^3. The double-helical complex was superimposed on a previously equilibrated box of pure water, and those solvent molecules that overlapped with the solute heavy atoms were removed. The system was equilibrated for 20 ps at 300 K, after which 300 ps of dynamics were calculated for data collection. In both simulations, long-range nonbonded forces were cut off between 10 and 12 Å using a switching function applied on a neutral group basis.[27] A dielectric constant of 1 was used in both calculations. In both simulations, energy was well-conserved and the temperature was stable throughout the data collection periods.

Results and Discussion

Vacuum Simulations. Figures 1 and 2 display the histories of each of the glycosidic torsion angles in both chains of the double helix from the vacuum simulation. As can be seen from the figures, transitions occurred on an infrequent basis in some of the torsion angles, while other angles remained almost in their initial conformations through much of the simulation. All except one of the ϕ angles for the (1→3) linkages (parts a, c, and e in both Figures 1 and 2) shifted from the starting conformation of −163° to around 90°, either during the heating and equilibration phase or shortly thereafter. Only case e of strand 2, the terminal linkage in that chain, remained in the starting conformation. The values of ψ for the same (1→3) linkages (parts f, h, and j of Figures 1 and 2) for both strands tended to shift from the starting conformation of −159° to a stable conformation around −140°. In most of these linkages the shift occurred during the heating and equilibration period. Only in the terminal linkages (part j of both figures) was there a significant tendency to remain in the starting conformation, although for both of these linkages, there were periods spent in the other conformation. For the (1→4) linkages of both strands, the ϕ angles (parts b and d of Figures 1 and 2) tended to remain near 180°, although exhibiting some significant fluctuations, while the ψ angle had two more distinctly separated stable states approximately 80° apart.

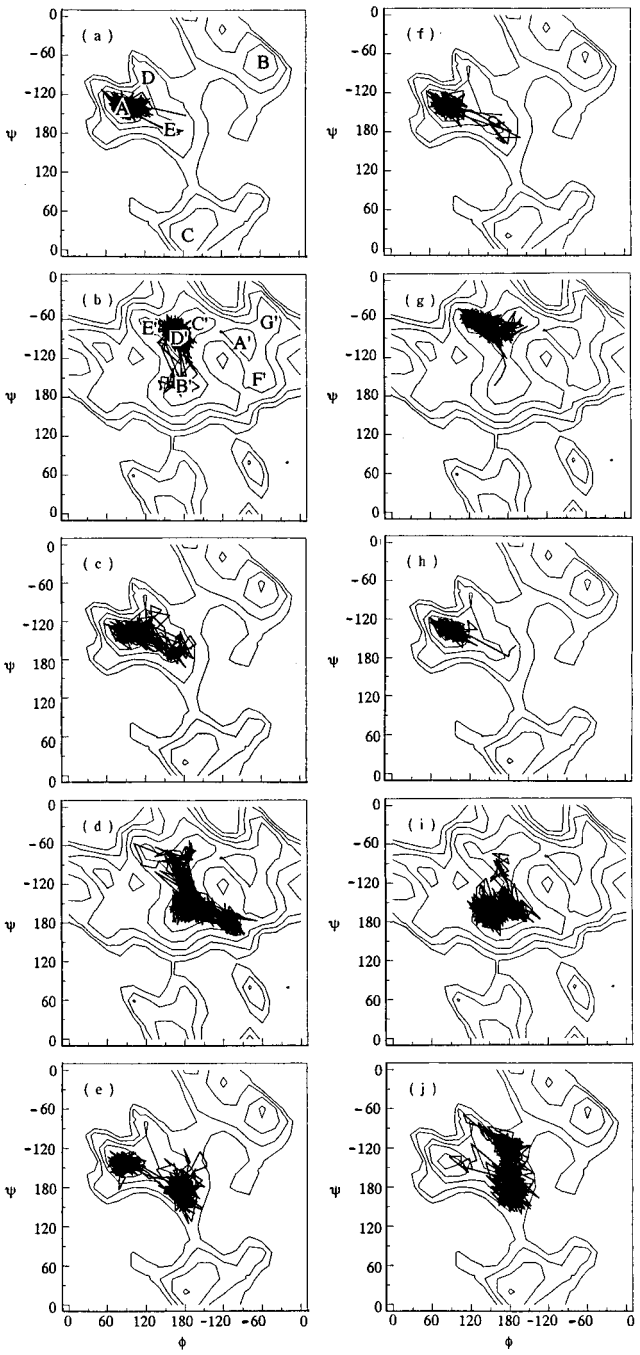

Figure 3. Trajectories of the linkage angles of strand 1 (a−e) and strand 2 (f−j) in vacuum, superimposed on the adiabatic energy map: (a) A1(1→3)B2, (b) B2(1→4)A3, (c) A3(1→3)B4, (d) B4(1→4)A5, (e) A5(1→3)B6, (f) A′1(1→3)B′2, (g) B′2(1→4)A′3, (h) A′3(1→3)-B′4, (i) B′4(1→4)A′5, (j) A′5(1→3)B′6.

In previous papers[19,20] we have reported the adiabatic Ramachandran conformational energy surfaces[28] for these two disaccharide linkages calculated using the same force field employed here, and these maps can be used to help interpret the observed trajectories for the individual linkages. Figure 3 displays the trajectories for each disaccharide linkage in both strands superimposed onto the appropriate conformational energy map. In the case of the neocarrabiose-like (1→3)

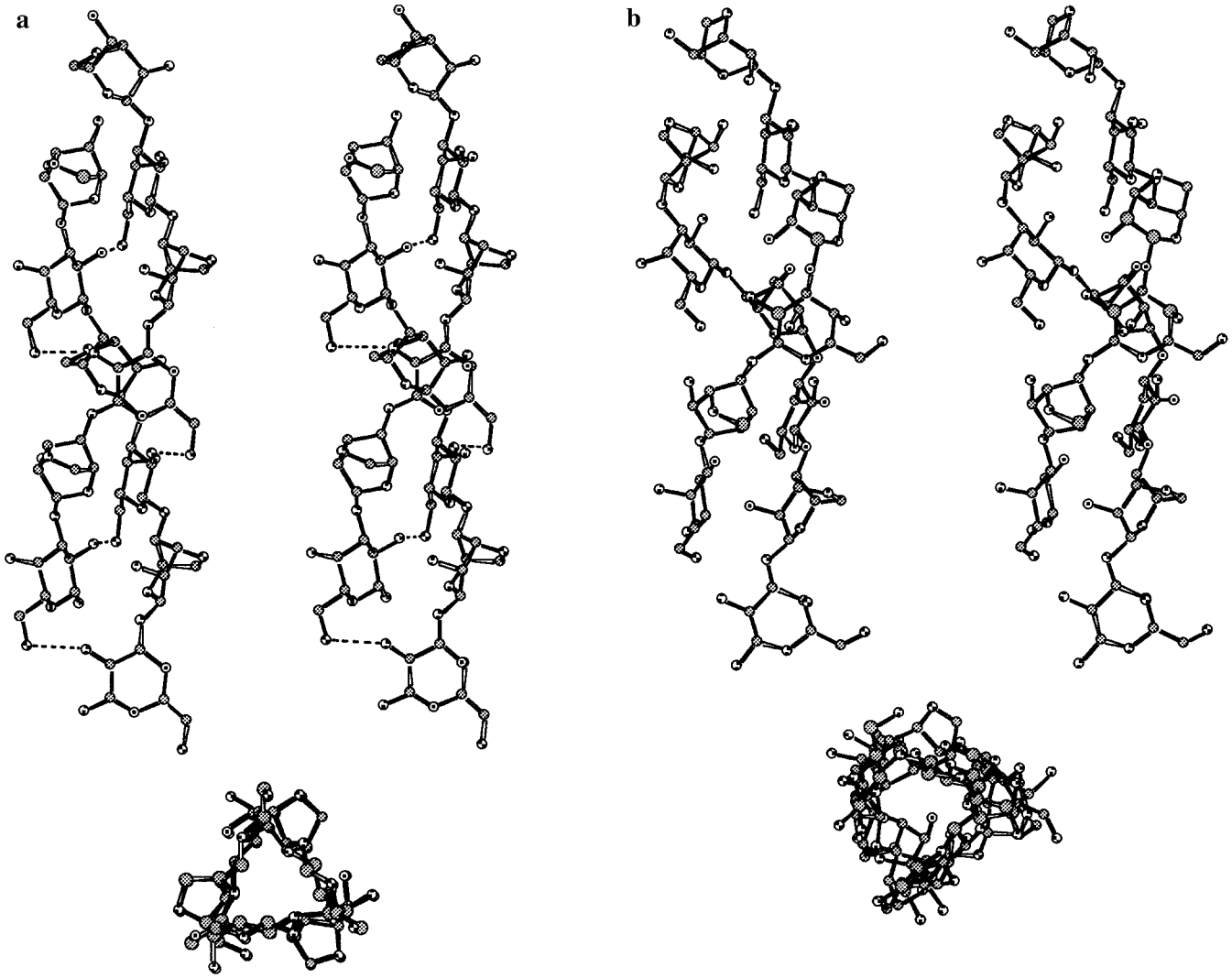

Figure 4. Stereo pair showing the initial (a) double-helical β-carrageenan hexamer conformation (side and top views) and after the 520 ps of vacuum dynamics (b). Interchain hydrogen bonds are shown as dashed lines in the initial figure.

linkages, the proposed fiber structure does not correspond to a minimum on the calculated vacuum surface,[19] and vacuum simulations of neocarrabiose tended to undergo a conformational shift away from the fiber structure to the global minimum-energy structure at (81°, −141°). As can be seen from Figure 3, such transitions also occurred for each of the (1→3) linkages of the double helix. In the first linkages, at the nonreducing end of the chains, the linkage adopted the vacuum global minimum-energy geometry and made at best only very brief visits back to the fiber conformation. For the middle linkage, there was a clear preference for the global minimum-energy conformation, but in strand 1 there were several returns to the fiber conformation that lasted for significant periods of time. For the two linkages of this type at the reducing end of the helices, the fiber structure appears to be favored. For these linkages (Figure 3e,j), strand 2 made only the briefest visit to the global minimum-energy well before returning to the fiber structure, where it oscillated between the experimental fiber structure and the crystal structure for the disaccharide at (−145°, −98°). In chain 1 this linkage made an extended transition to the global minimum-energy conformer but then returned to the fiber structure. Since all linkages made at least one transition, and most made several, it seems unlikely that these linkages are kinetically trapped in unfavorable conformations.

The situation was found to be somewhat different for the (1→4) linkage. On the adiabatic energy map for the corresponding carrabiose disaccharide, the proposed fiber structure is close to a significant local minimum at (−177°, −162°), which was found to be one of several neighboring minima of very similar energies clustered together in a horseshoe-shaped valley with only small barriers separating the different positions.[20] The global minimum at (−86°, −92°), labeled A in our previous study[20] (A′ in Figure 3b), is only 0.3 kcal/mol lower in energy than the well labeled B′ containing the fiber structure. Between these two wells are two other minima that were labeled C′ and D′ at (−154°, −59°) and (179°, −79°), respectively. Three other somewhat higher-energy minima are also located close to this low-energy valley, creating an extensive low-energy region allowing a fair degree of conformational flexibility, and MD simulations of carrabiose disaccharides in vacuum found that the molecules tended to explore all of the wells in this region. As can be seen from Figure 3 (parts b, d, g, and i), these linkages were somewhat less flexible in the double-helical hexamers. In the oligomers these linkages tended to explore only the central portion of the low-energy region, wells B′−D′−C′, and none made any transitions over to the global minimum-energy conformation A′. In both strands, the first linkage, toward the nonreducing end of the chains, favored the C′−D′ region while the second linkages at the reducing end of the chains tended to favor the fiber conformation.

Figure 4a displays a stereo pair of the structure of the hexamer double helical fragment in the proposed fiber diffraction conformation and Figure 4b displays a similar instantaneous "snapshot" of the conformations of these two chains at the end of the entire 520 ps of vacuum MD simulation. The fiber conformation is stabilized by hydrogen bonds between the O2 and O6 hydroxyl groups of β-D-galactose residues in different chains, which are indicated in the figure by dashed lines. There are five such hydrogen bonds between the chains in the hexamer double helix. The figure also includes an "end-on" view of the double helix to illustrate the 3-fold symmetry of this conformation. As can be seen from Figure 4b, the net effect of the various conformational transitions for the glycosidic linkages of the chains in the vacuum MD simulations discussed in the previous paragraphs was to distort the double helix, but overall the dimer complex remained a double helix throughout the simulation. Somewhat greater distortions occurred at the top of the chain, since as observed above, most of the transitions away from the fiber conformation also occurred in the residues closest to the nonreducing end of the chains. The stability of the double helix apparently was maintained in part by the interchain hydrogen bonds, most of which remained intact throughout the simulation. Figure 5 illustrates the history of these five hydrogen bonds through the use of a short vertical bar for each instantaneous step where the hydrogen bond was present, separated in each figure according to which hydroxyl group of the pair was the proton donor. The presence of the hydrogen bond in any particular structure was evaluated using a geometric criteria that required an oxygen−oxygen distance of 3.5 Å or less and an O−H···O angle of 120° or greater.[29] As can be seen, while all but one of these hydrogen bonds experienced some disruption, all were relatively stable and still present at the end of the simulation. The last two bonds experienced the most lability, both exchanging donor−acceptor identity frequently as well as breaking altogether for extended periods of the simulation.

Solution Simulations. Figure 6 displays the instantaneous conformations of the two hexamer chains at the end of the 320-ps simulation in aqueous solution. This conformation would appear qualitatively to be very different from the conformations shown in Figure 4, in that there seems to have been a significant unraveling of the double helix at the nonreducing end. This change is further illustrated by the end-on view at the bottom of the figure, where nearly all of the 3-fold regularity of the fiber starting structure has been lost. Figure 7 displays the trajectories of each of the disaccharide linkages in both chains projected onto the Ramachandran energy maps as in Figure 3. Paradoxically, most of these linkage trajectories are much more stable in the solution simulation than in the vacuum calculation, making only tightly restricted oscillations around the fiber starting conformation. None of the linkages in the first hexamer chain made any transitions at all, in sharp contrast to the many transitions made by both types of linkages in the vacuum simulation. As a result, chain 1 is substantially still in its fiber starting conformation. Essentially all of the unraveling of the double helix is due to conformational transitions in the first two residues of the second chain of the dimer (see Figure 7f,g). As can be seen for the individual histories of the two glycosidic torsion angles for both of these linkages (Figure 8), the (1→4) linkage made a significant conformational transition early into the simulation, to the region around (78°, −111°), and never returned. On the carrabiose vacuum adiabatic energy map, this conformation is some 4−6 kcal/mol higher in energy than the experimental conformation.[20] The first (1→3) glycosidic linkage

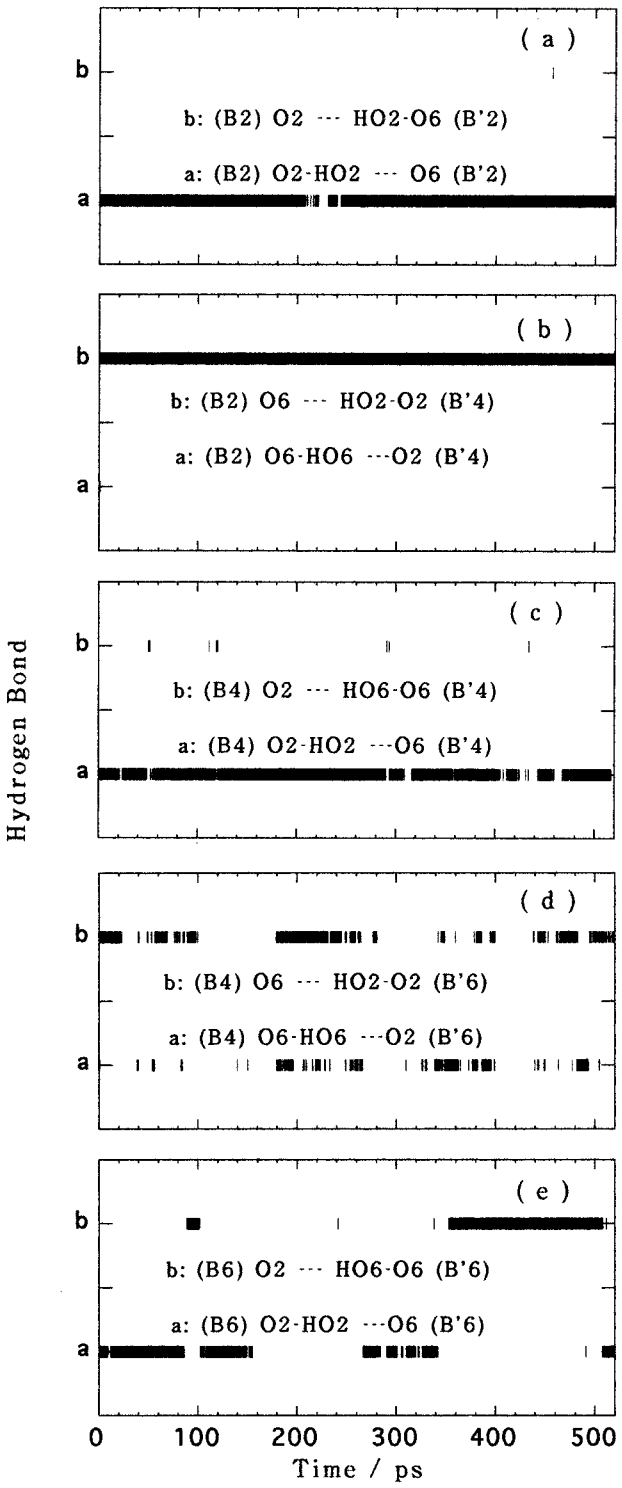

Figure 5. History of the occurrence of interchain hydrogen bonds in the vacuum trajectory.

made several transitions away from the starting structure, but returned to it at least once, before ending near the crystal structure of neocarrabiose. The transitions in these two linkages produced the unraveling seen in Figure 6. As with the first chain, the other three linkages of this oligomer were much more restricted in their conformational fluctuations and remained close to the starting fiber structure. The change in conformation seen in Figure 6 appears large but is actually fairly small in terms of physically observable quantities; both the radius of gyration of the complex and the end-to-end distances of the two strands

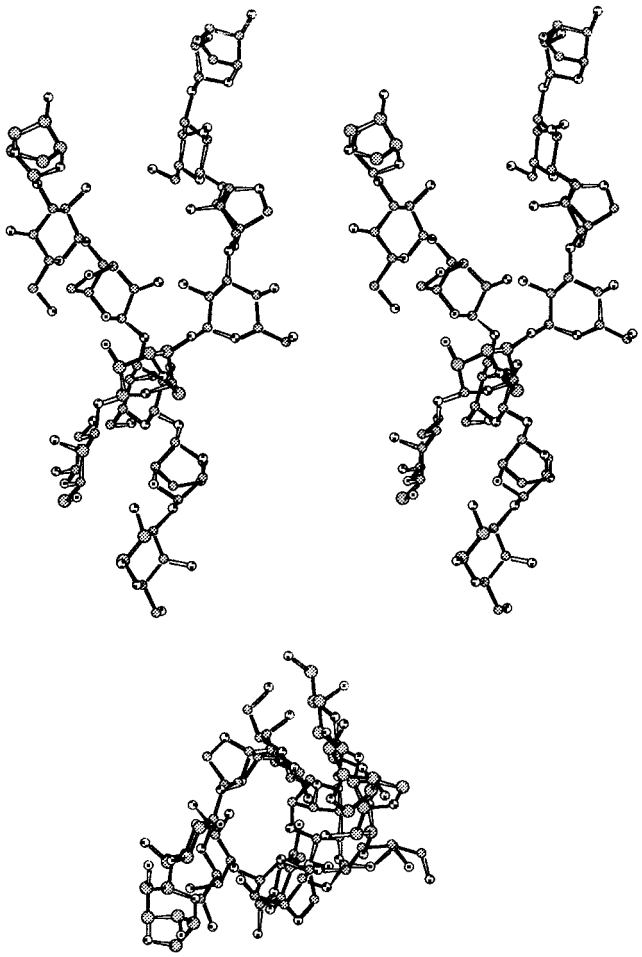

Figure 6. Stereo pair showing the final conformation of the β-carrageenan hexamer dimer after 320 ps of solution dynamics.

changed only very slightly from the beginning to the end of the simulation.

As was noted above, the proposed double-helical fiber conformation is stabilized by interchain hydrogen bonds,[4] which persisted throughout the vacuum MD simulation. However, the vacuum conditions of that simulation are highly artificial and provide no alternative to these hydrogen bonds, each of which would require considerable energy to disrupt. (The transition to the global minimum for the (1→3) linkage does allow for an intrachain hydrogen bond between the O2 groups of the β-D-galactose and 3,6-anhydro-α-D-galactose residues, replacing the interchain hydrogen bond.) In solution, the interchain hydrogen bonds can easily be broken if the hydroxyl groups involved make alternate bonds to water molecules. In the simulations, it was found that all five of these stabilizing hydrogen bonds were substantially disrupted. Figure 9 displays the histories of the five interchain hydrogen bonds of the fiber conformation in the same manner as in Figure 5. Two of these bonds exchanged early in the simulation and either did not reform or returned only very briefly. Two more were present for some short extended periods but did not exist for the overwhelming majority of the simulation. Only the hydrogen bond at the reducing end of the double helix was present for the majority of the simulation, although it too experienced repeated disruptions. This observed exchange of the interchain hydrogen bonds in solution suggests that carrageenan is not a double helix in solution since the hydrogen bonds required to stabilize it in this arrangement apparently are not themselves favored under these conditions.

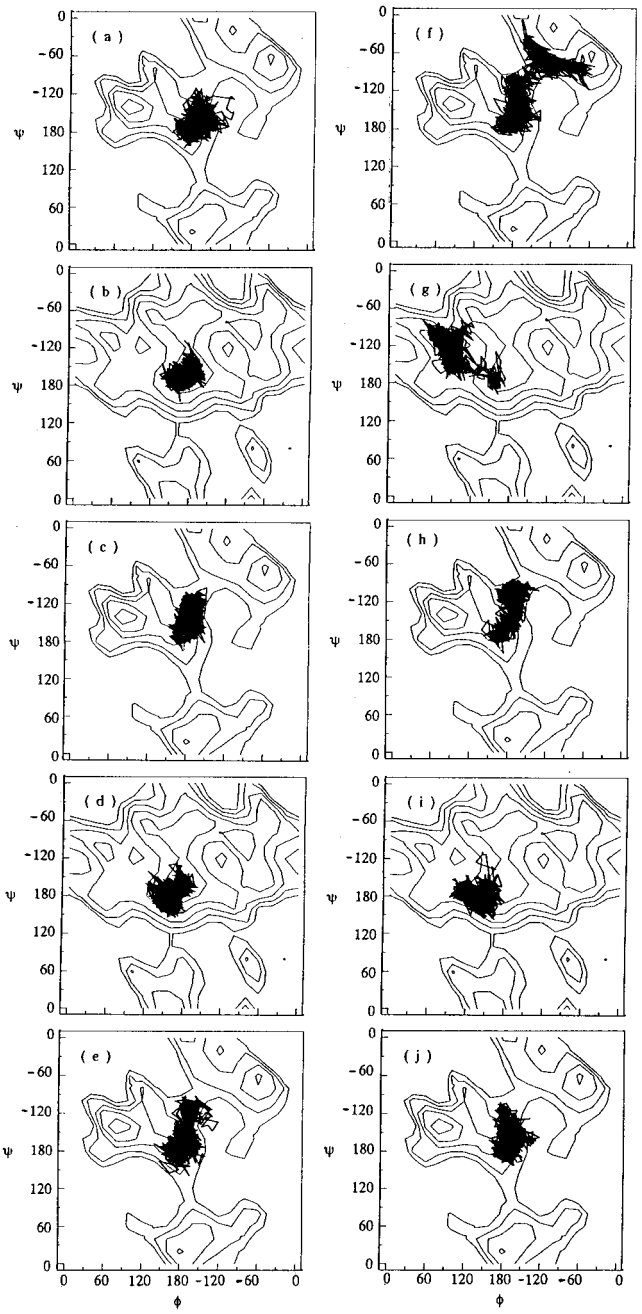

Figure 7. Trajectories of the linkage angles of strand 1 (a−e) and strand 2 (f−j) in water, superimposed on the adiabatic energy map. The order of the figures is the same as shown in Figure 3.

In our previous studies of neocarrabiose,[19] the intramolecular hydrogen bond in vacuum between the O2 hydroxyl groups of the two sugar rings that artificially stabilized the global minimum-energy structure was replaced in solution by hydrogen bonds to solvent, allowing the experimental conformation to be more stable. For the majority of the simulation time these hydrogen bonds were both made to a single water molecule that bridged between the two hydroxyl groups, stabilizing the experimental conformations, whose ϕ and ψ angles place these two hydroxyl groups at the proper distance to allow such bridging. Similar water bridging was observed in the present simulations as well. Table 1 lists the percentage of the trajectory time during which such water bridging was observed for each neocarrabiose-like linkage of both chains in the double-helix simulation in solution for the first 20 ps of heating and equilibration and for the final 20 ps of the simulation, calculated

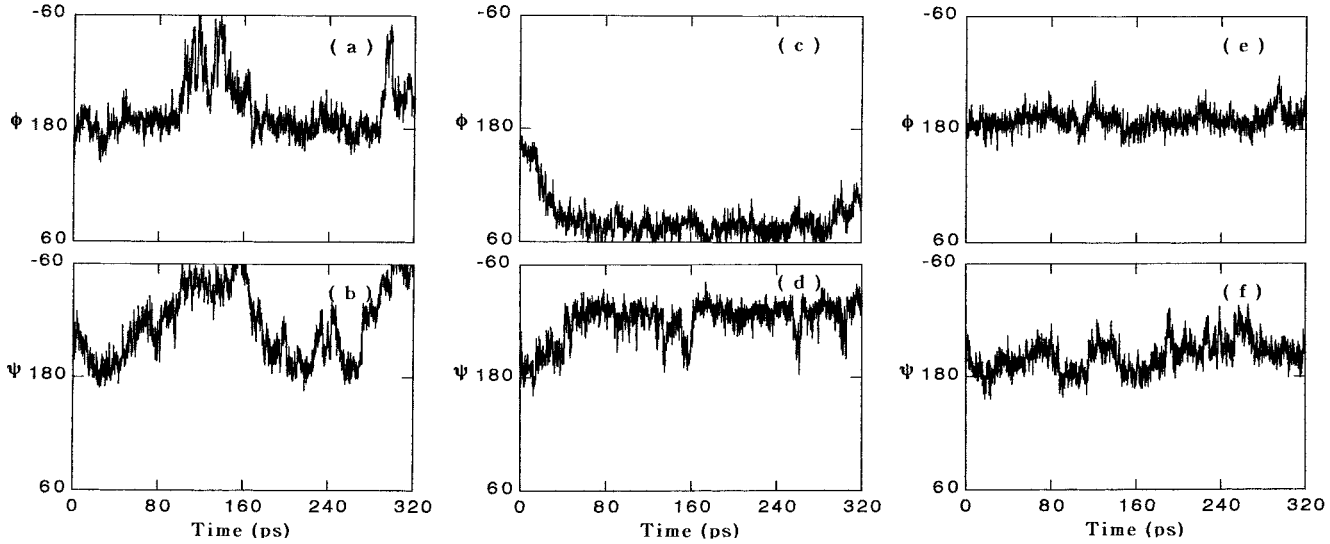

Figure 8. (a) and (b) Histories of a typical set of dihedral angles ϕ and ψ of strand 2 in the solution simulation (corresponding to the trajectory of the A′1(1→3)B′2 linkage, part f of Figure 7); (c) and (d) histories of the B′2(1→4)A′3 linkage angles of trajectory g of Figure 7; (e) and (f) histories of the linkage angles of trajectory j in Figure 7.

using the same geometric criteria employed for the interchain hydrogen bonds. As in the neocarrabiose simulation, the O2 hydroxyl groups on either side of each of the (1→3) linkages of both chains were bridged by a water molecule for the majority of the first 20 ps of the simulation, and all but one of these linkages was so bridged during the final 20 ps of the simulation as well. The one exception was the first such linkage of the second chain, which underwent the unraveling conformational transition discussed above, which resulted in these two hydroxyl groups being too far apart for a single water molecule to hydrogen bond to both.

Table 2 lists the total number of hydrogen bonds formed to water by each oxygen atom of both chains, calculated using the same geometric criteria as before. These are also compared to the number of hydrogen bonds to solvent observed in the previous simulations of neocarrabiose.[19] The total average number of hydrogen bonds to solvent during the first 20 ps of the simulation was 124.9 and during the final 20 ps was 124.1, showing that the degree of hydration did not increase during the unraveling of the double helix (this analysis ignores the water molecules hydrating the nonpolar portions of the polymer, which also contribute to the total hydration number of the chains). These results indicate that the individual strands are well-hydrated without separating, particularly once the interchain hydrogen bonds exchange. This in turn might suggest that any driving force for the separation of the chains is mainly entropic rather than an increase in the hydration enthalpy.

Although the simulations reported here were extremely costly to perform, requiring more than 3.5 CPU months on an IBM RS/6000 computer, it is clear from the results that if it were possible much longer simulation times, perhaps on the order of several nanoseconds, would be required to settle the questions raised by these preliminary calculations. It is extremely interesting that the double helix appears to have begun to unravel, particularly in light of recent experiments which indicate that this molecule is a single rather than a double helix in solution. However, the observed unraveling was the result of conformational transitions in only the first two disaccharide linkages of one of the two chains. Owing to the short simulation time, it is not clear whether the chain would have returned to the original conformation at a later time or whether more transitions in other linkages of the oligomer would have occurred. In this context, it is quite interesting that the other chain remained in the starting conformation throughout the simulation and actually appeared to be more stable in this conformation than the corresponding vacuum simulation, in spite of the fact that nearly all of the interchain hydrogen bonds that stabilize this complex in the proposed double-helical fiber diffraction structure are disrupted.

One possible interpretation of this observation might be that the simulation is of insufficient duration and that, given enough time, this chain would also have made significant conformational transitions. However, it is also possible that each individual chain could be stable in the proposed fiber conformation, but as a single helix rather than as a double-helix complex. The tightly constrained conformational fluctuations of the (1→3) linkages in the first oligomer resemble those of the previously studied neocarrabiose disaccharide in solution, where the fiber conformation was found to be the preferred conformer in solution even in the absence of any interchain hydrogen bonds as are proposed to exist in the double helix. The reason for the stability of this conformation was found to be that it resulted in a separation distance for two hydroxyl groups on opposite rings, which was optimal for a single water molecule to bridge between them by hydrogen bonding to both. Exactly similar hydrogen bonds are observed in the present double-helix calculation, and the presence of the dimer partner does not seem to interfere with their formation. At least for the limited duration of the simulation, the absence of the interchain hydrogen bonds does not seem to destabilize the helical conformation of the first chain, although it may be kinetically trapped in a higher-energy local conformational state. Thus it is possible that the conformation of an individual carrageenan chain in solution may be close to that proposed for the double-helical complex, but without the need for the second strand with its stabilizing hydrogen bonds. Without the interchain hydrogen bonds, there would seem to be little reason for the chains to associate, and the simulations provide no indication of any stabilizing interactions that could compensate for the entropic cost of forming a double helix.

Even if longer simulation times should find that the hexasaccharide dimer studied here is not stable as a double helix, this finding would not in itself prove that β-carrageenan does not exist in solution as a double helix, since six residues may

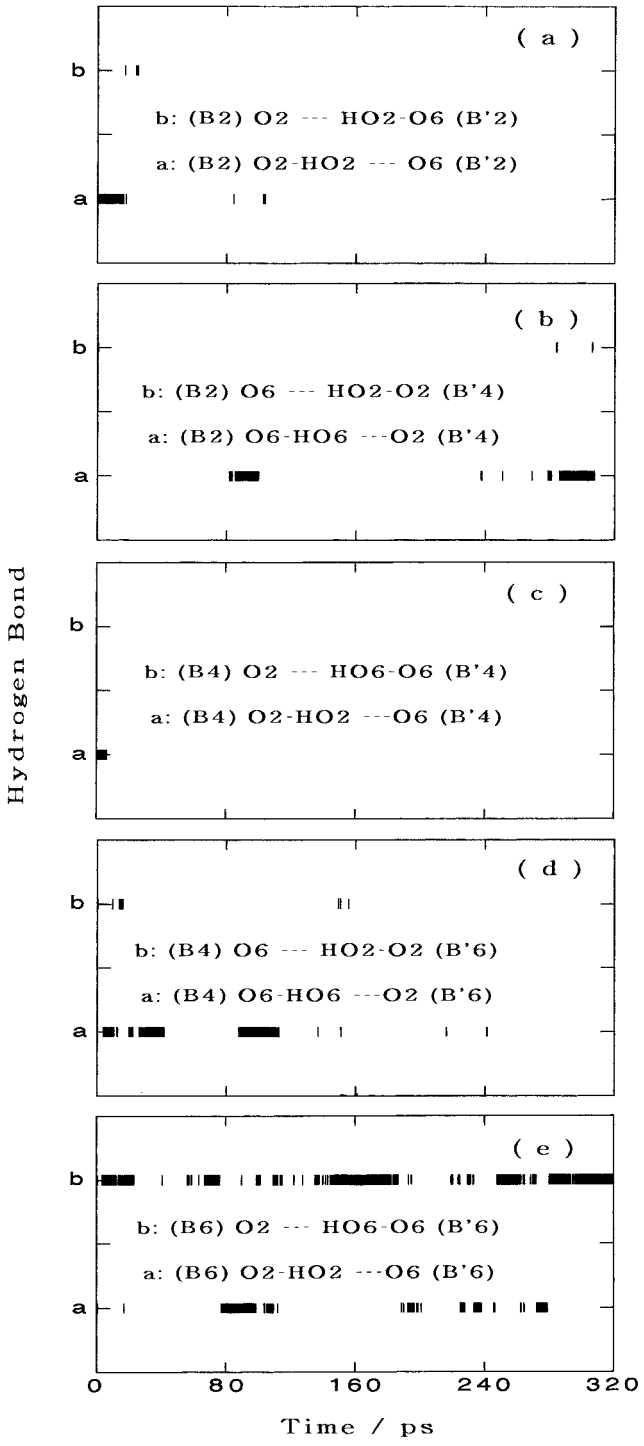

Figure 9. History of the occurrence of interchain hydrogen bonds in the solution trajectory.

well be below the critical polymer length required for a helix−coil transition to a stable helix.[30,31] However, in spite of the unraveling observed in the solution trajectory, these simulations also provide examples of long-term stability of the first helix, even in the absence of its dimer partner for half of its length and in the absence of its hydrogen bonds for its entire length. It is quite possible that if the unraveling continued to the point of complete separation of the two chains that the second chain would also adopt the helical conformation, which seems to be favored, at least for the (1→3) linkages, by the water molecules making hydrogen bond bridges between adjacent rings. Three of the four (1→4) linkages also seem to strongly favor the helical conformation in the solvated chains, further implying that this conformation may be stable in solution even as a single helix. Regardless of whether the chains favor a single or a double helix in solution, no evidence was found in the simulations to imply that the preferred conformation would be that of a random coil.

Some additional uncertainty arises from the choice of potential function. While it is a facile criticism that the results of simulations may be dependent on the choice of force fields, it has often been observed that in many situations, physical properties are not sensitively dependent on the exact details of the force fields, as long as the energy functions are qualitatively correct.[20,32−36] Some properties, however, may indeed be quite sensitive to the choice of force field, and hydrogen bond

TABLE 1: Percentage of Time in the Solution Trajectory during Which Water Molecules Bridged between the O2 Hydroxyl Groups of the (1→3) Linkages by Hydrogen Bonding to Both Groups, Indicated for Two 20-ps Intervals, at the Beginning and End of the Simulation

hydroxyl group pairs	percent of the indicated interval during which the hydroxyl groups were bridged by a water molecule	
	0−20 ps	300−320 ps
A1O2···B2O2	56.8	50.8
A3O2···B4O2	78.3	85.3
A5O2···B6O2	78.3	85.8
A′1O2···B′2O2	86.5	0.0
A′3O2···B′4O2	69.5	82.3
A′5O2···B′6O2	82.5	69.0

TABLE 2: Average Number of Hydrogen Bonds between Water and Sugar Oxygen Atoms, Calculated for the Initial 20 ps of the Trajectory and the Final 20 ps

strand 1				strand 2				neo-
residue	atom	0−20 ps	300−320 ps	residue	atom	0−20 ps	300−320 ps	carrabiose
A1	O1	1.6	0.9	A′1	O1	2.2	1.1	1.0
	O2	3.7	3.2		O2	4.5	3.7	2.8
	O4	4.4	3.6		O4	4.1	2.6	
	O5	1.1	0.8		O5	2.0	0.9	0.7
	O6	2.1	1.1		O6	2.3	1.5	1.0
	total	12.9	9.6		total	15.1	9.8	
B2	O1	0.8	1.1	B′2	O1	1.2	1.2	2.9
	O2	1.1	2.6		O2	3.8	1.5	2.7
	O4	2.6	2.6		O4	4.4	2.7	2.5
	O5	0.6	1.1		O5	1.2	1.3	0.8
	O6	2.3	2.1		O6	2.6	3.0	2.9
	total	7.4	9.5		total	13.2	9.7	
A3	O1	1.0	1.2	A′3	O1	1.1	1.1	
	O2	2.5	3.1		O2	2.8	2.7	
	O5	0.3	0.9		O5	0.5	0.6	
	O6	1.1	1.1		O6	1.1	1.2	
	total	4.9	6.3		total	5.5	5.6	
B4	O1	1.1	2.2	B′4	O1	0.8	1.0	
	O2	1.3	2.5		O2	1.5	3.0	
	O4	2.7	2.0		O4	2.6	2.4	
	O5	1.0	1.7		O5	0.8	1.2	
	O6	3.5	3.0		O6	2.5	3.6	
	total	9.6	11.4		total	8.2	11.2	
A5	O1	2.2	2.6	A′5	O1	1.1	1.6	
	O2	4.2	4.7		O2	2.5	2.7	
	O5	1.7	1.6		O5	0.3	1.1	
	O6	2.3	2.7		O6	1.1	1.7	
	total	10.4	11.6		total	5.0	7.1	
B6	O1	3.0	3.0	B′6	O1	2.4	2.4	
	O2	4.5	4.1		O2	2.9	2.3	
	O4	4.3	4.5		O4	3.1	3.5	
	O5	1.3	2.0		O5	2.1	1.5	
	O6	4.3	4.8		O6	4.8	4.2	
	total	17.4	18.4		total	15.3	13.9	

exchange is probably one such property, since small errors in water−water, sugar−sugar, or sugar−water hydrogen bond energies could significantly affect the equilibrium. Thus, the observed solvent stabilization of the helical conformation for the (1→3) linkages in these simulations could possibly be due to the choice of potential. It is encouraging, however, that similar solvent structuring in other sugar solutions has been found not to depend sensitively on the choice of water potential energy function,[36] and it is also encouraging that in the present case the apparently stable conformation is in accord with the experimental evidence.

Conclusions

The present simulations would seem to support the possibility that carrageenan is not a double helix in aqueous solution. While the simulation times are too short to reach definitive conclusions, the double-helix starting structure does appear to be unraveling during the course of the calculation. The six residue chains may also be too short in length to support helical conformations, but the apparent stability of many of the linkages in helical conformations, in accord with the previously observed stability of these linkage conformations in disaccharides in aqueous solution, would seem to imply that the individual strands adopt the previously predicted helical conformation, but that these separate helices do not intertwine as double helices. In the vacuum control simulation, the individual glycosidic linkages were able to make transitions away from the fiber structure without completely disrupting the double helix, which remained qualitatively intact, apparently owing to the persistence of the interchain hydrogen bonds stabilizing the dimer. The observed relative stability of the dimer in vacuum would be consistent with the existence of such a double helix under relatively anhydrous conditions, as in a fiber. However, in solution these interchain hydrogen bonds are not stable, and the hydroxyl groups that make these bonds are accessible to solvent even in the dimer and might be expected to hydrogen bond to water. The results of these simulations are thus in accord with experimental data for both fiber and solution conditions. While the great expense of the simulations currently precludes extending the trajectories, probably calculations of only three or four times the length of the present study could resolve much of the uncertainty. Given the rapid developments in computer technology, the prospects seem quite good that such a simulation will be possible in the near future, and similar simulations of chains double or triple the length of the present oligomers should be possible within a decade.

Acknowledgment. The authors are grateful to S. Paoletti, A. Cesàro, and R. Urbani for helpful discussions. This work was supported by NSF Grant CHE-9307690 to J.W.B. K.U. would like to thank Daicel Chemical Co. (Japan) for a travel grant to support his visit to Ithaca.

References and Notes

(1) Kennedy, J. F. *Carbohydrate Chemistry*; Clarendon Press: Oxford, 1988.
(2) Anderson, N. S.; Campbell, J. W.; Harding, M. M.; Rees, D. A.; Samuel, J. W. B. *J. Mol. Biol.* **1969**, *45*, 85−99.
(3) Arnott, S.; Scott, W. E.; Rees, D. A.; McNab, C. G. A. *J. Mol. Biol.* **1974**, *90*, 253−267.
(4) Millane, R. P.; Chandrasekaran, R.; Arnott, S.; Dea, I. C. M. *Carbohydr. Res.* **1988**, *182*, 1−17.
(5) McKinnon, A. A.; Rees, D. A.; Williamson, F. B. *Chem. Commun.* **1969**, 701−702.
(6) Norton, I. T.; Goodall, D. M.; Morris, E. R.; Rees, D. A. *J. Chem. Soc., Faraday Trans. 1* **1983**, *79*, 2501−2515.
(7) Rochas, C.; Rinaudo, M. *Biopolymers* **1980**, *19*, 1675−1687.
(8) Rochas, C.; Rinaudo, M. *Biopolymers* **1984**, *23*, 735−745.
(9) Snoeren, T. H. M.; Payens, T. A. J. *Biochim. Biophys. Acta* **1976**, *437*, 264−272.
(10) Smidsrod, O.; Grasdalen, H. *Carbohydr. Polymers* **1982**, *2*, 270−272.
(11) Paoletti, S.; Smidsrod, O.; Grasdalen, H. *Biopolymers* **1984**, *23*, 1771−1794.
(12) Grasdalen, H.; Smidsrod, O. *Macromolecules* **1981**, *14*, 229−231.
(13) Vanneste, K.; Mandel, M.; Paoletti, S.; Reynaers, H. *Macromolecules* **1994**, *27*, 7496−7498.
(14) Hjerde, T.; Smidsrod, O.; Christensen, B. E. *Carbohydr. Res.* **1996**, *288*, 175−187.
(15) Lamba, D.; Segre, A. L.; Glover, S.; Mackie, W.; Sheldrick, B.; Peréz, S. *Carbohydr. Res.* **1990**, *208*, 215−230.
(16) Tvaroska, I.; Rochas, C.; Taravel, F.-R.; Turquois, T. *Biopolymers* **1992**, *32*, 551−560.
(17) Urbani, R.; Blas, A. D.; Cesàro, A. *Int. J. Biol. Macromol.* **1993**, *15*, 24−29.
(18) Ueda, K.; Ochiai, H.; Imamura, A.; Nakagawa, S. *Bull. Chem. Soc. Jpn.* **1995**, *68*, 95−106.
(19) Ueda, K.; Brady, J. W. *Biopolymers* **1996**, *38*, 461−469.
(20) Ueda, K.; Brady, J. W. *Biopolymers* **1997**, *41*, 323−330.
(21) Brooks, B. R.; Bruccoleri, R. E.; Olafson, B. D.; Swaminathan, S.; Karplus, M. *J. Comput. Chem.* **1983**, *4*, 187−217.
(22) Ha, S. N.; Giammona, A.; Field, M.; Brady, J. W. *Carbohydr. Res.* **1988**, *180*, 207−221.
(23) Verlet, L. *Phys. Rev.* **1967**, *159*, 98−103.
(24) van Gunsteren, W. F.; Berendsen, H. J. C. *Mol. Phys.* **1977**, *34*, 1311−1327.
(25) Jorgensen, W. L.; Chandrasekhar, J.; Madura, J. D.; Impey, R. W.; Klein, M. L. *J. Chem. Phys.* **1983**, *79*, 926−935.
(26) Durell, S. R.; Brooks, B. R.; Ben-Naim, A. *J. Phys. Chem.* **1994**, *98*, 2198−2202.
(27) Tasaki, K.; McDonald, S.; Brady, J. W. *J. Comput. Chem.* **1993**, *14*, 278−284.
(28) Brady, J. W. *Adv. Biophys. Bioeng.* **1990**, *1*, 155−202.
(29) Brady, J. W.; Schmidt, R. K. *J. Phys. Chem.* **1993**, *97*, 958−966.
(30) Flory, P. J. *Principles of Polymer Chemistry*; Cornell University Press: Ithaca, NY, 1953.
(31) Flory, P. J. *Statistical Mechanics of Chain Molecules*; Interscience: New York, 1969.
(32) Ha, S. N.; Madsen, L. J.; Brady, J. W. *Biopolymers* **1988**, *27*, 1927−1952.
(33) Kouwijzer, M. L. C. E.; van Eijck, B. P.; Kroes, S. J.; Kroon, J. *J. Comput. Chem.* **1993**, *14*, 1281−1289.
(34) Brady, J. W. In *Carbohydrates: Structures, Dynamics & Syntheses*; Finch, P., Ed.; Blackie Academic & Professional: Glasgow, 1998.
(35) Glennon, T. M.; Zheng, Y.-J.; Grand, S. M. L.; Shutzberg, B. A.; Merz, K. M. *J. Comput. Chem.* **1994**, *15*, 1019−1040.
(36) Liu, Q.; Brady, J. W. *J. Phys. Chem.* **1997**, *B101*, 1317−1321.